Supplementary Materials

Critical Role of Acetylation in Tau-Mediated Neurodegeneration and Cognitive Deficits

Sang-Won Min, Xu Chen, Tara E Tracy, Yaqiao Li, Yungui Zhou, Chao Wang, Kotaro Shirakawa, S. Sakura Minami, Erwin Defensor, Sue Ann Mok, Peter Dongmin Sohn, Birgit Schilling, Xin Cong, Lisa Ellerby, Bradford W. Gibson, Jeffrey Johnson, Nevan Krogan, Mehrdad Shamloo, Jason Jestwicki, Eliezer Masliah, Eric Verdin*, and Li Gan*

*Correspondence: lgan@gladstone.ucsf.edu, eric.verdin@gladstone.ucsf.edu

Supplementary Table-1

Supplementary Figures 1–10

Min et al. Supplementary Table 1

AD Human Brain Samples Used in This Study

Case number	Braak	Gender	Age	Tangles	Plaque Load (# plaques/mm2/temporal gyrus)
2010	0	M	70	None	0
900	0	F	79	None	0
1036	0	M	93	None	0
872	0	F	75	None	0
1248	0	M	83	None	0
325	0	F	86	None	0
1339	0	F	70	None	2.3
1004	1	M	75	None	0
684	1	F	84	None	0
1213	1	M	74	None	0
842	1	F	83	None	0
332	1	F	94	None	13.2
546	2	F	80	None	0
776	2	M	95	None	0
1040	2	F	74	None	0
1039	2	M	85	None	0
541	2	M	75	Sparse	2.4
884	2	F	81	None	6
347	2	F	84	None	15.2
38	2	M	84	Sparse	11.2
1229	3	F	91	None	0
82	3	F	86	None	0
1012	3	F	98	None	6.8
523	3	F	82	None	8
111	3	F	93	Sparse	10.2
375	5	F	87	Sparse	17.2
941	5	M	88	Sparse	5.6
675	5	F	85	Sparse	18.4

Mount Sinai Samples from Bm-22 (*superior temporal gyrus*)

Min et al., Supplementary Figure 1 (related to Fig. 1)

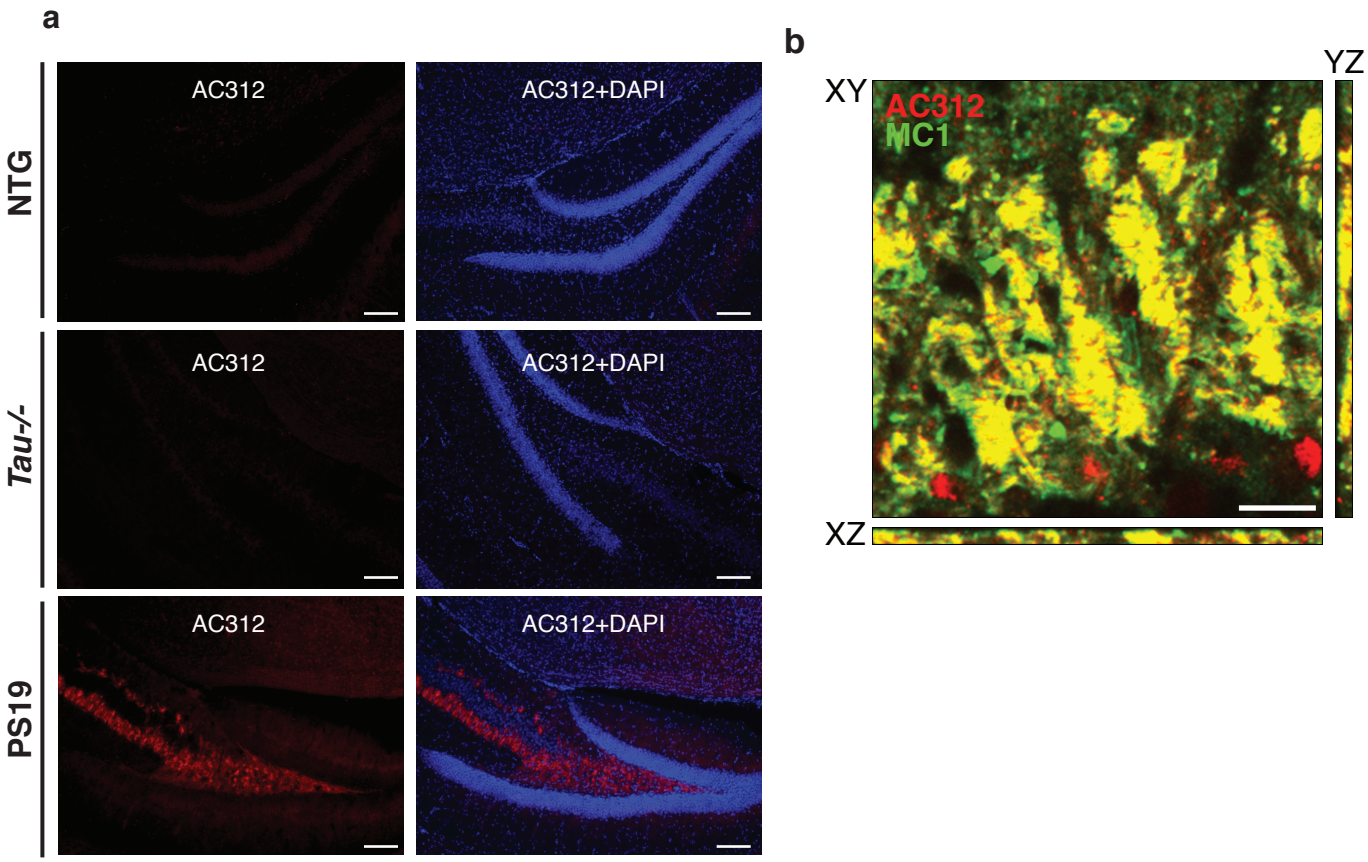

Supplementary Fig. 1. AC312 immunoreactivity is specific for human tau and colocalizes with MC1 signal.
(a) AC312 immunoreactivity was only detectable in the hippocamal region of PS19 mice, but not detectable in Non-transgenic (NTG) or *Tau–/–* controls. Scale bar: 250 µm.
(b) Representative orthogonal view of colocalization of AC312 and MC1. z-stacks images were rendered for orthogonal view with image J software. Scale bar: 10 µm.

Min et al. Supplementary Figure 2 (related to Figure 2)

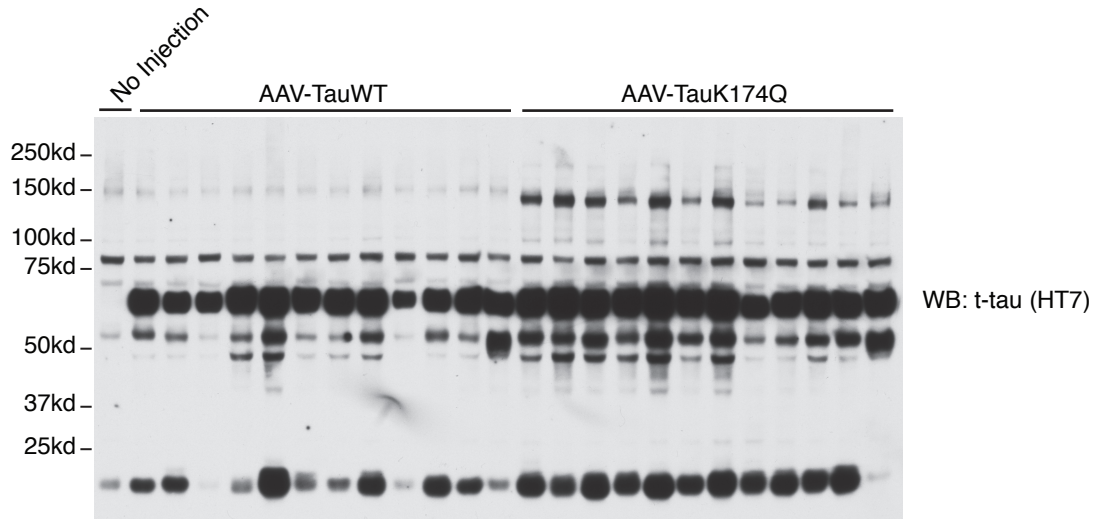

Supplementary Fig. 2. Representative immunoblot of hippocampal lysates injected with AAV-TauWT or TauK174Q by HT7.
AAV-TauK174Q induced significantly higher amount of tau dimers than AAV-TauWT.

Min et al., Supplementary Figure 3 (related to Figure 2)

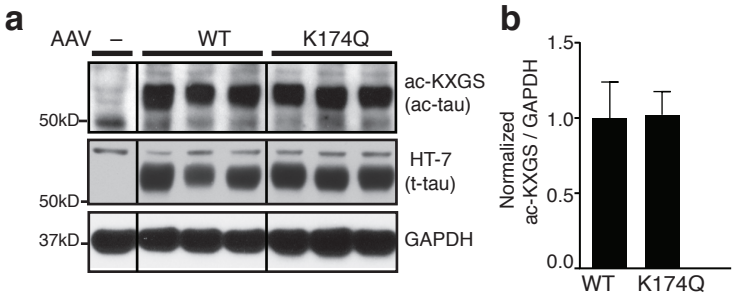

Supplementary Fig. 3. Acetylation on KXGS motif is not altered by K174Q mutation.
(a) Representative immunoblot of lysates from hippocampi injected with AAV-TauWT or TauK174Q with ac-KIGS tau antibody, HT7 (t-tau) and GAPDH.
(b) Quantification of levels of ac-KIGS tau normalized with GAPDH. n=11 (WT), n=9 (K174Q). unpaired student t-test. Values are means ± SEM (b)

Min et al. Supplementary Figure 4 (related to Figure 2)

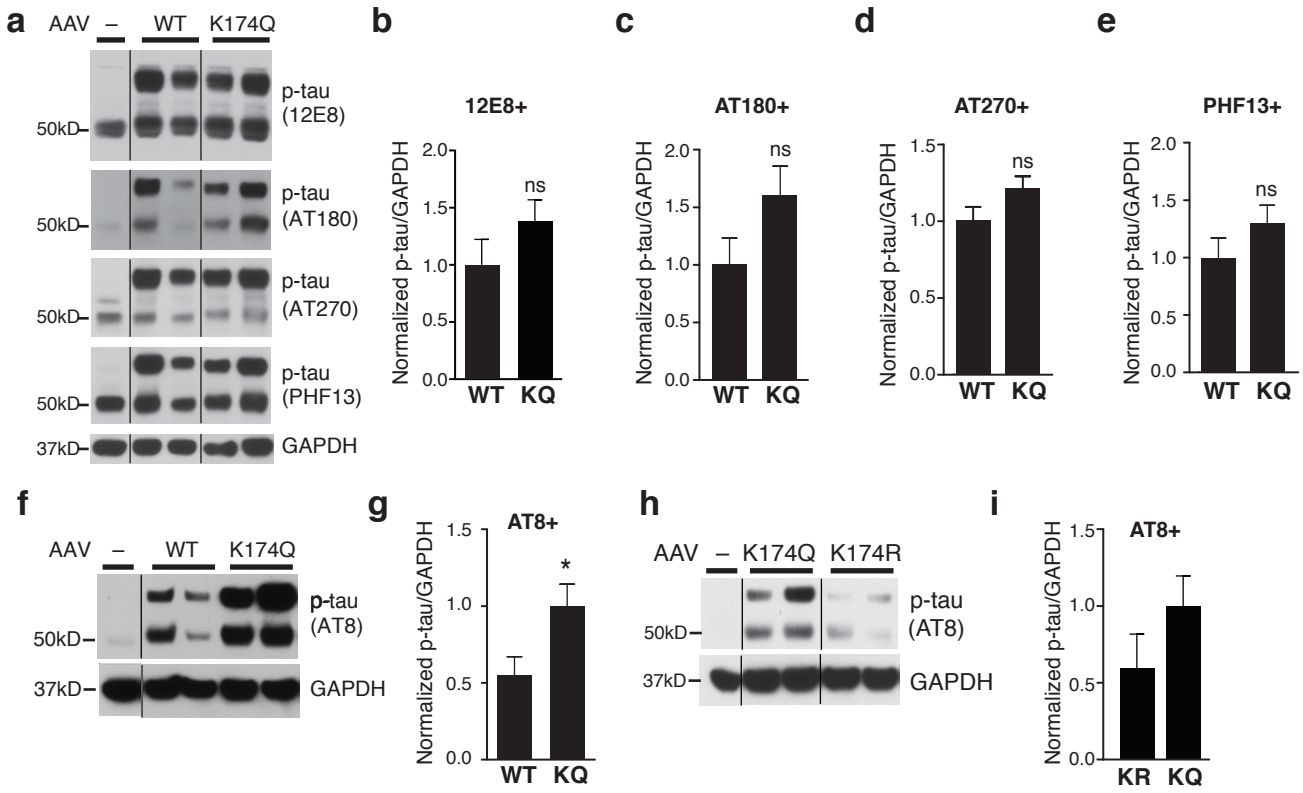

Supplementary Fig. 4. K174Q mutation enhances the levels of AT8-positive p-tau.
(a–e) Effects of K174Q expression on a panel of p-tau antibodies. (a) Representative immunoblot of hippocampal lysates injected with similar amount of AAV-TauK174Q or TauK174R with12E8, AT180, AT270, PHF13 antibodies. Quantification of 12E8 (b), AT180 (c), AT270 (d), and PHF13 (e) immunoblots. n=11 (WT), n=12 (K174Q), ns, non-significant.
(f–i) K174Q expression elevated levels of AT8-positive p-tau. Representative immunoblot of hippocampal lysates injected with similar amount of AAV-TauWT andTauK174Q (f) or AAV-K174R and AAV-K174Q (h) and detected with AT8 antibody. Quantification of AT8-positive immunopositive signal (g, i) n=11 (WT), n=12 (KQ),n=9 (KR), *, p <0.05, unpaired student t test. Values are means ± SEM (b-e,g,i)

Min et al. Supplementary Figure 5 (related to Figure 4)

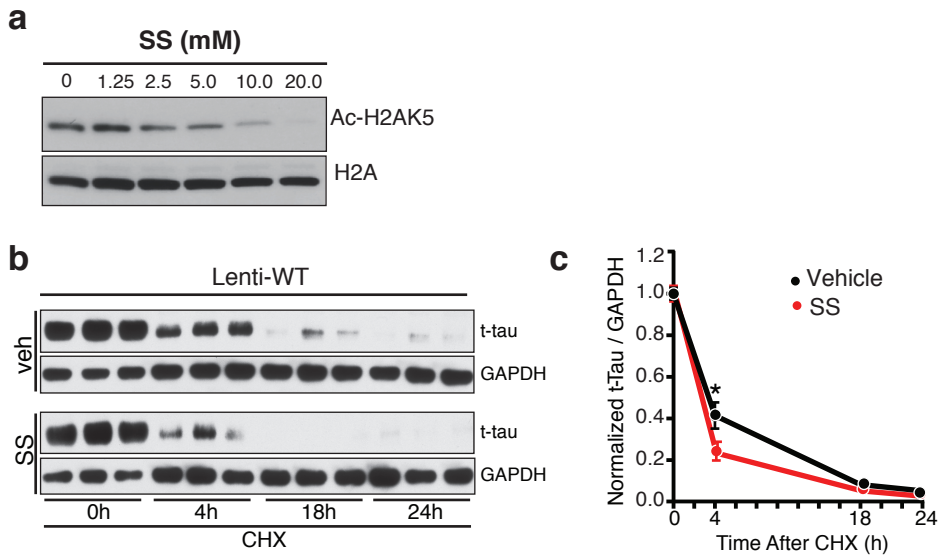

Supplementary Fig. 5. Salicylate inhibits p300 in HEK cells and expedited tau turnover in primary neurons infected with lenti-WT hTau.

(**a**) Immunoblot showing that treatment of HEK293 cells with salicylate (SS) lowered levels of ac-H2AK5 in a dose-dependent manner.

(**b**) Representative immunoblot showing the turnover of human WT tau pretreated with vehicle or salicylate (5 mM) during 24h period CHX treatment. (**c**) Quantification of the turnover of human WT tau pretreated with vehicle or SS. n=11 from three independent experiments. * $p < 0.05$, unpaired student t-test. Values are means ± SEM (b).

Min et al., Supplementary Figure 6 (related to Figure 4)

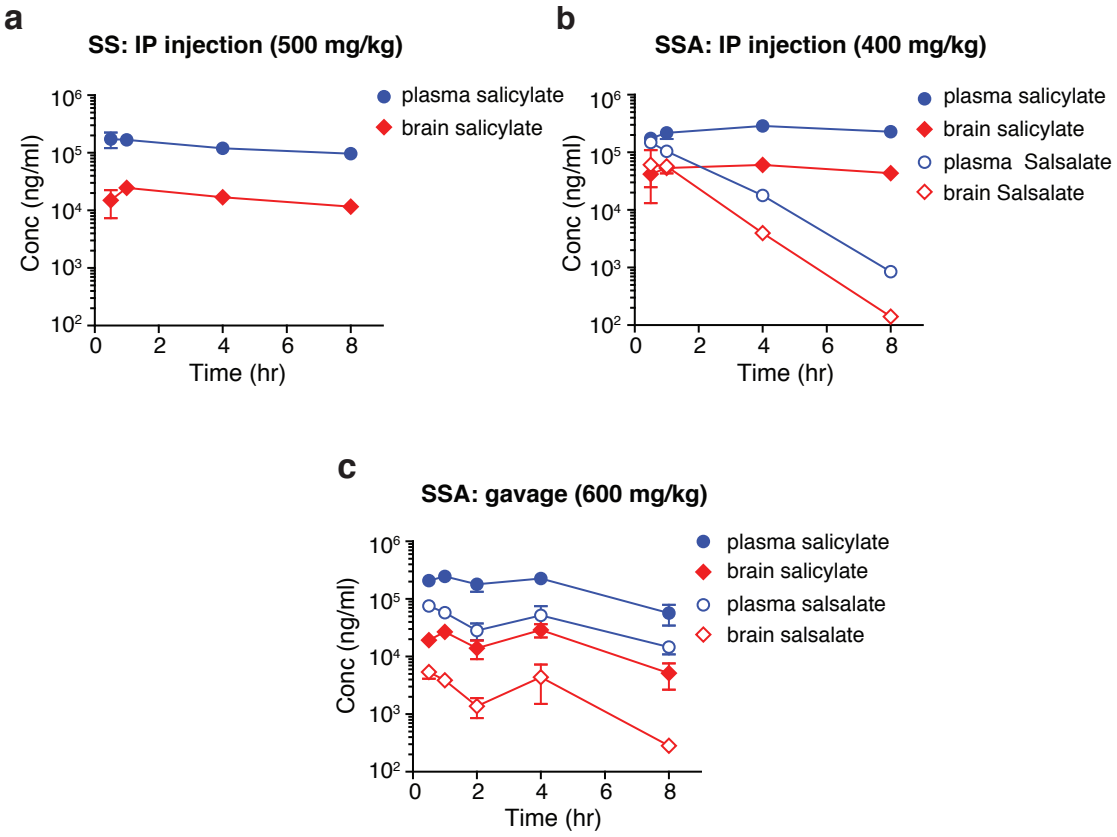

Supplementary Fig. 6. Pharmacokinetic (PK) analysis of salicylate and salsalate delivered via IP or gavage in mice. Concentrations of salicylate (SS) or salsalate (SSA) in the plasma or brain lysate over 8 hr were measured by HPLC-MS. **(a)** 500 mg/kg SS or **(b)** 400 mg/kg SSA was given via IP injection to wild-type C57B6 mice. n=2 mice/time point. **(c)** 600 mg/kg salsalate was given by gavage injection to wild-type C57B6 mice. n=3 mice/time point. Values are means ± SEM (a-c).

Min et al. Supplementary Figure 7 (related to Figure 4)

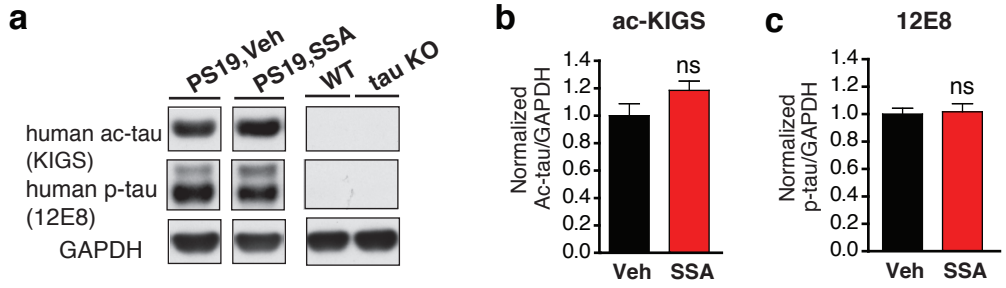

Supplementary Fig. 7. Salsalate treatment does not change levels of ac-tau (KIGS) or p-tau (S262) in the hippocampus of PS19 mice.

(**a**) Representative immunoblot of ac-tau (anti-ac-KIGS) and p-tau (anti-pS262/S356, 12E8) of hippocampal lysate from PS19 mice treated with vehicle or SSA. Vehicle-treated non-transgenic WT and tau KO mice were included as controls. Levels in vehicle-treated group were set as 1. n=8 mice/condition, 10-11 months old. (**b-c**) Quantification of ac-tau (KIGS) (b) and p-tau (S262/S356) (c) in hippocampal lysate from PS19 mice treated with vehicle or SSA. unpaired student t-test, ns= not significant. values are means ± SEM (b, c).

Min et al. Supplementary Figure 8 (related to Figure 5)

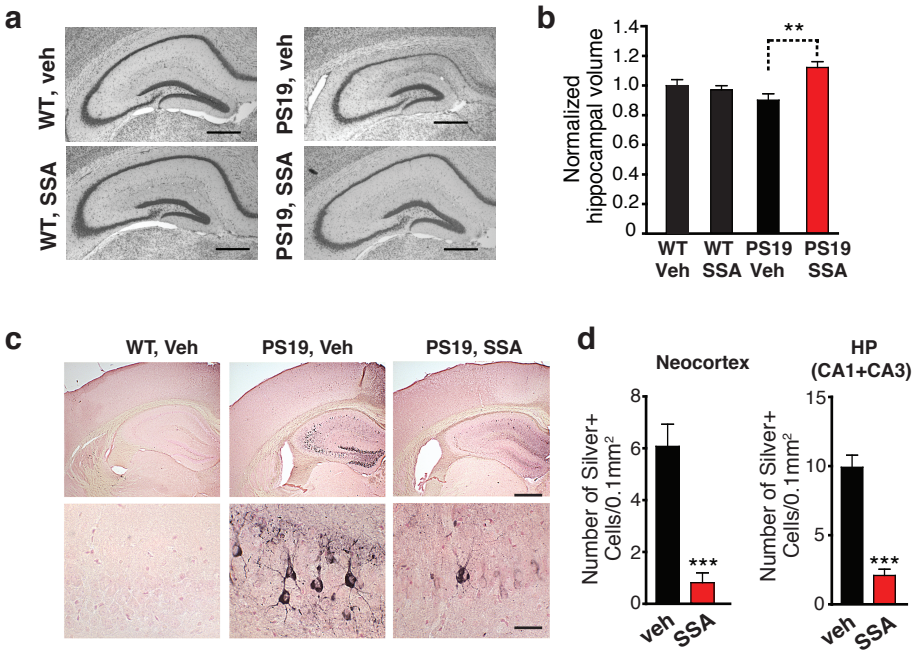

Supplementary Fig. 8. Protective effects of salsalate treatment in male PS19 mice.
(a) Representative nissl staining of hippocampus from vehicle-treated WT, SSA-treated WT, vehicle-treated PS19 and SSA-treated PS19 mice. Scale bar, 500 μm.
(b) Quantification of hippocampal volume in vehicle- or SSA-treated WT, and vehicle- or SSA-treated PS19 mice. n=11 (WT, veh), 14 (WT, SSA), 10 (PS19, veh), 9 (PS19, SSA), 9-10 months old, **p<0.01, one-way ANOVA, Tukey-Kramer post hoc analyses.
(c) Example of Gallyas staining images of vehicle-treated WT mice, and PS19 mice treated with vehicle or SSA. Scale bar: 250 μm (upper panel); 25 μm (lower panel).
(d) Quantification of silver-positive cells or neurites in neocortex and hippocampus (CA1+CA3) or vehicle- or SSA treated PS19 mice. ***p<0.001, unpaired student t-test. Values are means ± SEM (b, d).

Min et al. Supplementary Figure 9 (related to Figure 6)

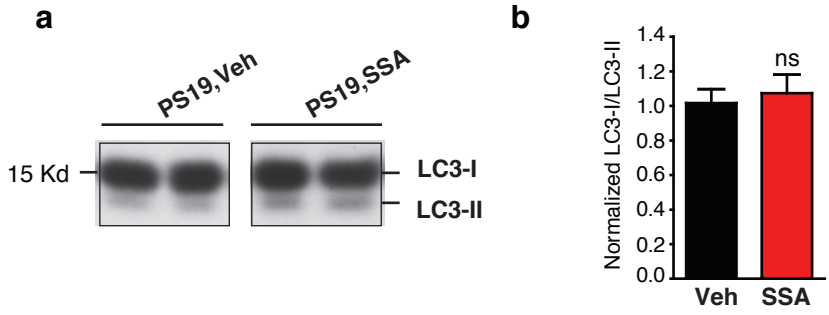

Supplementary Fig. 9. Salsalate treatment did not significantly alter the levels of LC3-II in the brains of PS19 mice.

(a) Representative immunoblot of LC3-I and LC3-II in cortical lysates from PS19 mice treated with vehicle or SSA.

(b) Quantification of ratio of LC3-I/LC3-II in cortex lysate from PS19 mice treated with vehicle or SSA. Levels in vehicle-treated group were set as 1. n=12 (veh), 10 (SSA), 10–11-month old. unpaired student t-test, ns= not significant. values are means ± SEM (b).

Min et al. Supplementary Figure 10 (related to Figure 6)

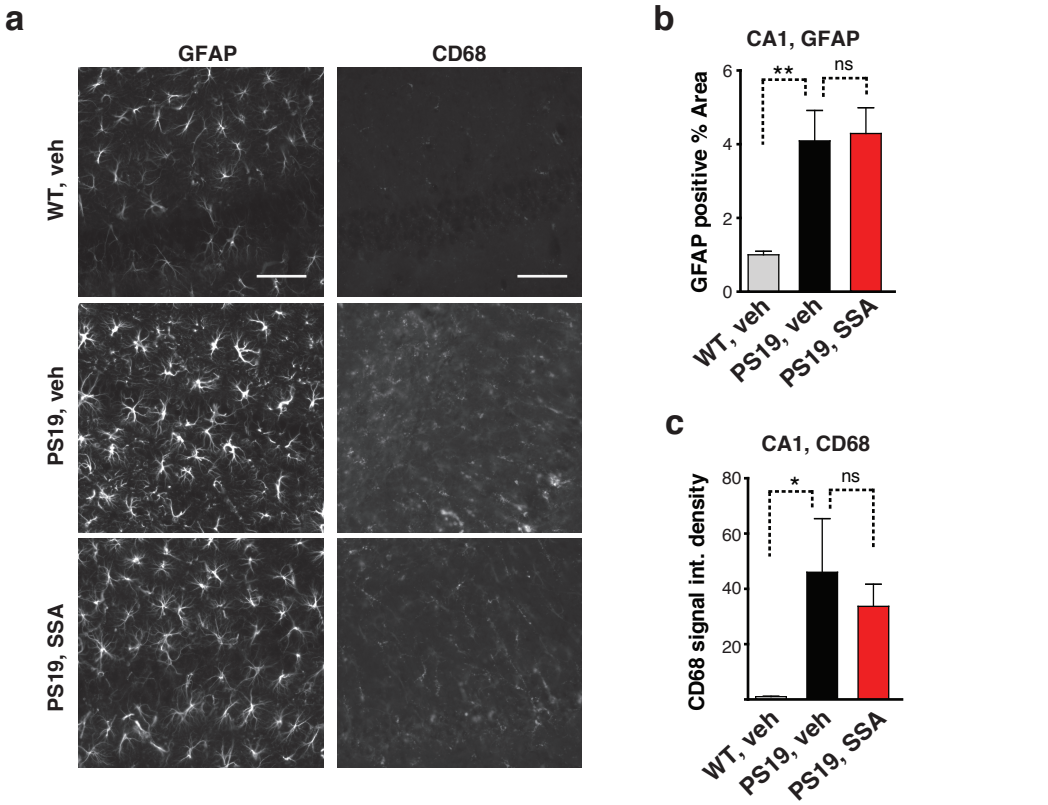

Supplementary Fig. 10. Salsalate treatment does not significantly affect astrogliosis and microgliosis in the brains of PS19 mice.

(a) Representative images of GFAP and CD68 fluorescent staining in the hippocampi (CA1) of WT mice treated with vehicle, PS19 mice treated with vehicle or SSA.
(b) Quantification of GFAP positive % area in the hippocampi (CA1).
(c) Quantification of integrated intensity of CD68 signals in the hippocampi (CA1).
n=9 (WT, veh), 7 (PS19, veh), 8 (PS19, SSA). 10-11 months old,
* $p < 0.05$, **, $p < 0.01$, ns= not significant, one –way ANOVA, Tukey-Kramer post-hoc analyses.
Values are means ± SEM (b, c). Scale bar: 50 μm.